Quasi-isotropic underwater acoustic carpet cloak based on latticed pentamode metafluid

Cite as: Appl. Phys. Lett. **114**, 094101 (2019); https://doi.org/10.1063/1.5085568
Submitted: 13 December 2018 . Accepted: 18 February 2019 . Published Online: 05 March 2019

Zhaoyong Sun, Xuecong Sun, Han Jia, Yafeng Bi, and Jun Yang

Applied Physics Letters ARTICLE scitation.org/journal/apl

Quasi-isotropic underwater acoustic carpet cloak based on latticed pentamode metafluid

Cite as: Appl. Phys. Lett. **114**, 094101 (2019); doi: 10.1063/1.5085568
Submitted: 13 December 2018 · Accepted: 18 February 2019 ·
Published Online: 5 March 2019

Zhaoyong Sun,[1] Xuecong Sun,[1,2] Han Jia,[1,3,a)] Yafeng Bi,[1] and Jun Yang[1,2,3,a)]

AFFILIATIONS

[1]Key Laboratory of Noise and Vibration Research, Institute of Acoustics, Chinese Academy of Sciences, 21 North 4th Ring Road, Beijing 100190, China
[2]School of Electronic, Electrical and Communication Engineering, University of Chinese Academy of Sciences, 19A Yuquan Road, Beijing 100049, China
[3]State Key Laboratory of Acoustics, Institute of Acoustics, Chinese Academy of Sciences, 21 North 4th Ring Road, Beijing 100190, China

[a)]**Authors to whom correspondence should be addressed:** hjia@mail.ioa.ac.cn and jyang@mail.ioa.ac.cn

ABSTRACT

We present a practical design of an underwater acoustic carpet cloak with 2-dimensional version of the pentamode lattice. The quasi-conformal transformation, which is achieved by inverse Laplace's equations with Neumann and Dirichlet boundaries, is used to obtain the required parameters of the impedance matching carpet cloak. The theoretical carpet cloak is pre-divided into 300 cells and then filled with the corresponding pentamode material unit cells to achieve the latticed pentamode carpet cloak. The simulation results indicate that the proposed carpet cloak has a good and broadband cloaking effect. Moreover, the technique in this work can also be used to design arbitrary shaped devices.

The transformation method, which is used to design amazing devices such as cloaks for wave controlling, was initially proposed for electromagnetic waves[1,2] and then generalized to acoustics.[3,4] It uses coordinate transformation to build connections between geometric space and material space.

One of the most attractive applications is the acoustic carpet cloak—an invisible device which can conceal the objects on a reflecting surface. The acoustic carpet cloak was first proposed by using the linear transformation method.[5] Since then, much interesting work on the acoustic carpet cloak has been reported.[6–11] However, the linear transformation always leads to great anisotropic parameters, which makes the carpet cloak difficult to be impedance matched with the background medium. Moreover, the shape of the cloaked space is also limited by the linear transformation. A potential approach for an arbitrary shaped and impedance matching acoustic carpet cloak is quasi-conformal transformation (QCT).[12,13] The QCT method requires that the material parameters are isotropic but vary continuously with the position. For underwater acoustic waves, this requirement, combining with impedance matching, is still very difficult to meet. An appropriate option is using a pentamode material (PM),[14] which can be completely fabricated from rigid solids in the practical case. The effective shear modulus is extremely smaller than the compressive moduli so that the PM has fluid-like properties. In addition, the effective density and modulus can be continuously tuned simultaneously. Thus, the PM is easy to be impedance matched with water. The PM has attracted great attention in mechanics and underwater acoustics.[15–25]

In this letter, we use a 2-dimensional (2D) version of PM lattice to design a broadband and impedance matching acoustic carpet cloak. The required parameters are obtained using the QCT method, which is achieved by solving inverse Laplace's equations with Neumann and Dirichlet boundaries.[13] The PM unit cells are designed by retrieving the energy bands,[20,25] and their effective parameters coincide with the desired ones well. The QCT method is reapplied to deform the regular PM unit cells to construct the carpet cloak. The simulation results show that the designed acoustic carpet cloak have good cloaking effects in a wide frequency range.

Considering that the virtual space and physical space are described by complex coordinates $w = u + iv$ and $z = x + iy$ respectively, the conformal transformation optics builds a relationship between those two spaces in the following way:[2]

$$n_z = n_w \left| \frac{dw}{dz} \right| = n_w \sqrt{\frac{1}{detJ}}, \tag{1}$$

where n_z and n_w denote the refractive index in physical and virtual spaces, respectively, and J is the Jacobian matrix. This result is derived by mapping the Helmholtz equation in physical space into the virtual space with the analytical function $w(z)$. Since the propagation of the acoustic wave in isotropic media also obeys the Helmholtz equation, the conformal transformation can also be used to design acoustic devices.[26,27] Thus, the relationship in Eq. (1) will still be kept in acoustics.

Conformal transformation provides the possibilities for isotropic carpet cloak design. Figure 1 shows the transformation of a carpet cloak. The virtual space *ABCDEF* presents the free space with refractive index n_w, while the physical space $A'B'C'D'E'F'$ represents the carpet cloak filled with the transformed media with refractive index n_z. Points A', B', C', D', E', and F' in the transformed space have the same coordinates as points A, B, C, D, E, and F in the virtual space, which means that line BC is mapped to curve $\overset{\frown}{B'C'}$ and other boundaries remain unchanged in the transformation. The background medium is water with density ρ_0, bulk modulus K_0, and refractive index $n_w = n_0$. According to Eq. (1), n_z is determined by the transformation matrix J. However, finding a suitable mapping $z(w)$ for the designed carpet cloak is still a great challenge. Quasi-conformal transformation is an appropriate option for this situation.[12,13] One way to realize QCT is calculating the inverse mapping $w(z)$ by numerically solving inverse Laplace's equations with predefined boundary conditions. The QCT theory suggests that the Cauchy-Riemann conditions must be satisfied in the mapping $w(z)$:

$$\frac{\partial u}{\partial x} = \frac{\partial v}{\partial y}, \tag{2a}$$

$$\frac{\partial u}{\partial y} = -\frac{\partial v}{\partial x}, \tag{2b}$$

which can result in the Laplace equations as follows:

$$\nabla^2 u = 0, \tag{3a}$$

$$\nabla^2 v = 0. \tag{3b}$$

According to the equivalence of the external boundaries between virtual and physical spaces, the Neumann and Dirichlet boundaries are used:

$$\vec{n} \cdot \vec{\nabla} u(x,y)|_{A'B'C'D',E'F'} = 0, \quad v(x,y)|_{A'B'C'D',E'F'} = y, \tag{4a}$$

$$\vec{n} \cdot \vec{\nabla} v(x,y)|_{F'A',D'C'} = 0, \quad u(x,y)|_{F'A',D'E'} = x. \tag{4b}$$

Thus, the inverse Jacobian matrix $A = J^{-1}$, which is shown as follows:

$$A = \begin{pmatrix} \frac{\partial u}{\partial x} & \frac{\partial u}{\partial y} \\ \frac{\partial v}{\partial x} & \frac{\partial v}{\partial y} \end{pmatrix}, \tag{5}$$

can be obtained by solving the Laplace equation (3) with the boundary equations (4) in a partial differential equation solver. Because the calculation is numerical, the matrix element $A_{11} = \partial u/\partial x$ ($A_{12} = \partial u/\partial y$) does not exactly equal to $A_{22} = \partial v/\partial y$ ($-A_{21} = -\partial v/\partial x$). This leads to slight anisotropy. Thus, the transformation can be regarded as quasi-conformal. In order to realize an impedance matching device, the density and bulk modulus of the physical space have to satisfy the properties shown as follows:

$$\rho = \frac{\rho_0 c_0}{c} = \rho_0 n = \rho_0 \sqrt{\frac{1}{detJ}}, \tag{6a}$$

$$K = \rho c^2 = \frac{K_0}{n} = K_0 \sqrt{detJ}. \tag{6b}$$

In this work, the side lengths of the designed cloak are $E'F' = 480$ mm and $D'E' = 208$ mm. The bottom side $\overset{\frown}{B'C'}$ is a curve described by $y = a\cos^2(\pi x/b)$ with $a = 30$ mm, $b = 347$ mm, and $-144\text{ mm} \leqslant x \leqslant 144$ mm. The background medium is water with $\rho_0 = 1000\ \text{Kg/m}^3$, $K_0 = 2.25$ GPa, and $n_w = n_0 = 1$. The inverse Jacobian matrix A is obtained by solving the Laplace equations (3) with the boundaries Eq. (4) by using a partial differential equation solver. Then, the inverse mapping $w(z)$ and the mapping $z(w)$ are confirmed. The refractive index profile in the device is shown in Fig. 2(a), which presents a petal-like distribution. The refractive index tends to 1, the value of water, near the boundary $D'E'$, $E'F'$, and $F'A'$. It reaches the maximum of 1.35 at the top point of curve $\overset{\frown}{B'C'}$ and the minimum of 0.75 near points B' and C'. In order to be realized by the PM structure, the cloak is pre-divided into 300 different cells, i.e., 15 rows and 20 columns. The refractive index in each cell is the area average of the continuous one. The discrete indexes are shown in Fig. 2(b). Thus, it is easy to obtain the required bulk modulus and density of each cell according to Eq. (6). Then, the main task is to find the PM unit cells that have effective parameters identical to the required ones.

A basic unit cell of PM is shown in Fig. 3(a) which is colored in light yellow. The substrate is aluminum with density $\rho_{Al} = 2700\ \text{kg/m}^3$, Young's modulus $E_{Al} = 69$ GPa, and Poisson's ratio $\nu = 0.33$. The regular hexagon cells have effective properties similar to isotropic fluids. The geometric parameters of the basic PM unit cell are characterized by side length l, structure thickness t, block size (s, h), and corner factor q. In the quasi-static regime,[28] the effective density is the volume

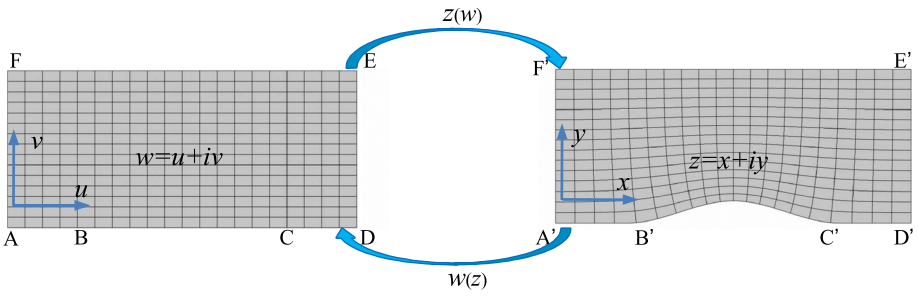

FIG. 1. Illustration of conformal transformation acoustics. Conformal mapping $\omega(z)$ transforms the virtual space *ABCDEF* into the physical space $A'B'C'D'E'F'$, while the inverse mapping $z(\omega)$ transforms the physical space back to the virtual space.

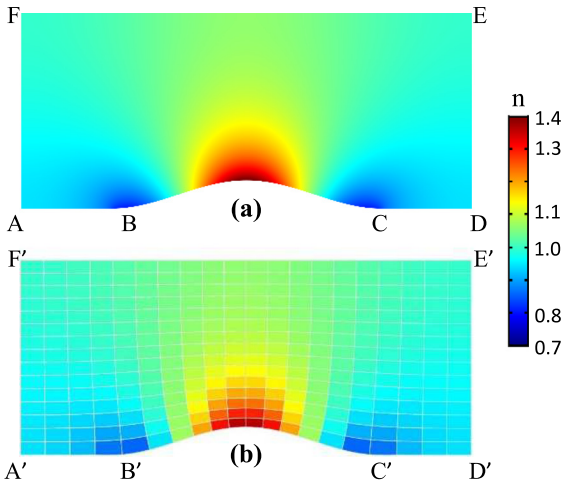

FIG. 2. Profile of (a) the continuous refractive index and (b) the discrete approximation in the acoustic carpet.

average of the mass and therefore mainly depends on the block size (s, h). The ratio of thickness and side length, $\eta = t/l$, mainly determines the effective bulk modulus of the PM. Thus, the properties of the PM lattice are primarily determined by the shape rather than the size of the structure. The effective parameters of the PM unit cell can be calculated by Bloch-Floquet analysis.[25,29] The required geometric parameters of the 300 cells are obtained by retrieving the energy bands.[20,25] A rectangle-like structure is formed by carefully tailoring the retrieved PM. It is named as the PM brick, which is colored in lemon as shown in Fig. 3(a). There are four different PM bricks in Fig. 3, where every brick has the side length of $l = 8$ mm. Figure 3(b) illustrates a 15×20 sized PM array built by these bricks. In the PM array, every PM brick has the same effective refractive index as that in the corresponding cell in Fig. 2(b). The cells in the red frame are the four PM bricks shown in Fig. 3(a).

Then, we use the QCT to deform the PM array into an appropriate shape, which can form the desired carpet cloak. Since QCT is approximately conformal, the angles and shapes are regarded as almost locally unchanged during the transformation. Thus, the effective parameters that mainly depend on the shape of the PM unit cell will not be affected seriously. A program is written to read the coordinates of the PM array and to transform the geometry by acting the transformation matrix J to these coordinates. Thus, the deformed PM array, i.e., the latticed PM carpet cloak (PMC), is acquired and shown in Fig. 3(d). It is obvious that the latticed PMC has the same shape as the designed carpet cloak shown in Fig. 2(b). The four PM bricks in the red frame of Fig. 3(b) are transformed into the structure in the red frame of Fig. 3(d). The enlarged version of the transformed structure is shown in Fig. 3(c). Comparing the structure in Fig. 3(c) with that in Fig. 3(a), we can notice that the shape of the transformed microstructure remains highly similar to that of the original one although the size of the structure has been changed considerably. This indicates that the effective parameters will not be influenced seriously. It can be seen that most of the PM unit cells in the latticed PMC keep the shape of a highly approximate regular hexagon lattice. Since the bottom boundary $\overset{\frown}{B'C'}$ is not specific, this technique can be used to build a carpet cloak with an arbitrarily shaped bottom boundary.

The performance of the latticed PMC is simulated using COMSOL Multiphysics. The results are shown in Fig. 4, where a Gaussian beam of frequency 15 kHz is incident at 55° from the left top side to the center of the bottom. The bottom side is set as the acoustic rigid boundary, while the other three are radiation boundary conditions. Figure 4(a) illustrates the empty field case, where the rigid bottom side imitates the rigid ground plane. It is obvious that the reflected waves retain the plane wave properties. In Fig. 4(b), the incident beam is scattered by the rigid bump on the plane. We can notice the feature of the scattered waves, i.e., two distinct beams at different angles. Figure 4(c) demonstrates the acoustic field distribution of the rigid bump covered with the theoretical cloak. The field is almost identical to that of the rigid plane shown in Fig. 4(a), which indicates the almost perfect performance of the theoretical cloak. Figure 4(d) shows the field distribution of the rigid bump with the latticed PMC. Even though there is a tiny lateral shift in the reflected field,[30] the reflected wave still retains a high similarity to that of the theoretical cloak in

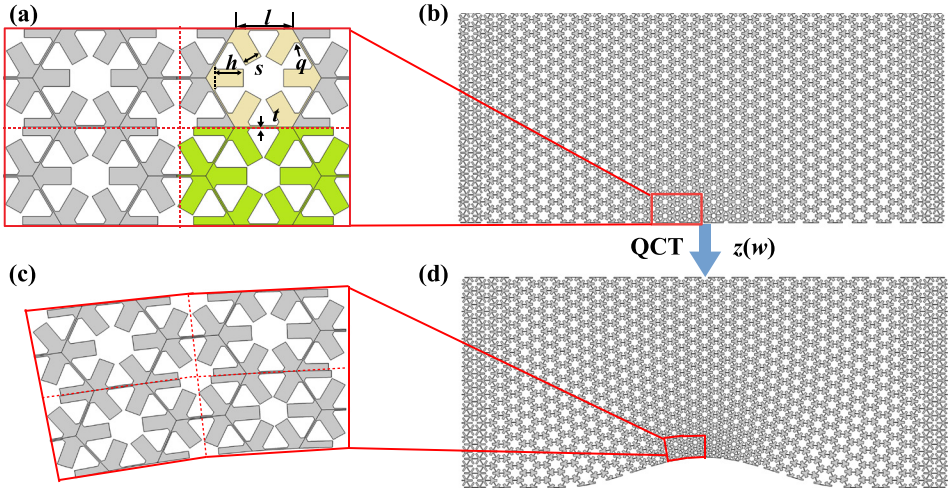

FIG. 3. (a) Microstructure of the 2D PM, with a basic PM unit cell colored in light yellow and a PM brick colored in lemon. (b) The 15×20 sized PM brick array. Every PM brick has the same effective refractive index as the index of the corresponding cell in Fig. 2(b). (c) The deformed PM bricks archived by conformally transforming the regular PM bricks shown in (a). (d) The latticed PMC transformed from the array shown in (b) with QCT.

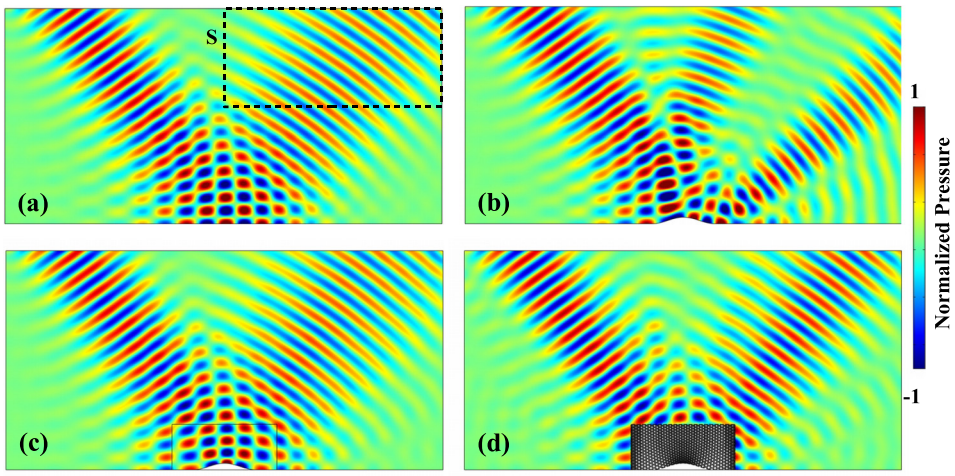

FIG. 4. Acoustic pressure field of (a) the rigid plane, (b) the rigid scatter, (c) the theoretical cloak, and (d) the latticed PMC at 15 kHz incident at 55°.

Fig. 4(b). Thus, it can be concluded that the latticed PMC can cloak the scatter well at 15 kHz.

Moreover, the cosine similarity index (CSI) is used to evaluate the performance of the proposed carpet cloak at different frequencies. The CSI is written as follows:[9]

$$CSI = \frac{\boldsymbol{P}^r \cdot \boldsymbol{P}^o}{|\boldsymbol{P}^r||\boldsymbol{P}^o|} = \frac{\Sigma P_i^r P_i^o}{\sqrt{\Sigma (P_i^r)^2}\sqrt{\Sigma (P_i^o)^2}}. \quad (7)$$

In Eq. (7), P^r is the pressure amplitude of the rigid plane (as reference values), while P_o denotes the pressure amplitude of the rigid scatter with or without the carpet cloak. The measure region, marked by the dashed line S in Fig. 4(a), is a 400 mm × 1000 mm rectangle area 600 mm above the bottom side. Figure 5 shows the CSIs in three different cases at the frequencies ranging from 10 kHz to 20 kHz. It can be seen that the CSIs of the theoretical PMC are almost 1, which means that the theoretical PMC has an identical performance to the rigid plane. The CSIs of the latticed PMC coincide with that of the theoretical PMC very well, while the CSIs of the rigid scatter are much smaller than those of the theoretical and latticed PMC. Thus, the latticed PMC is as effective as the theoretical one in a broadband frequency domain.

Furthermore, the case of the incoming beam incident in the vertical direction is also studied. The simulation results are shown in Fig. 6, where the scattered pressure fields for different cases are presented. It

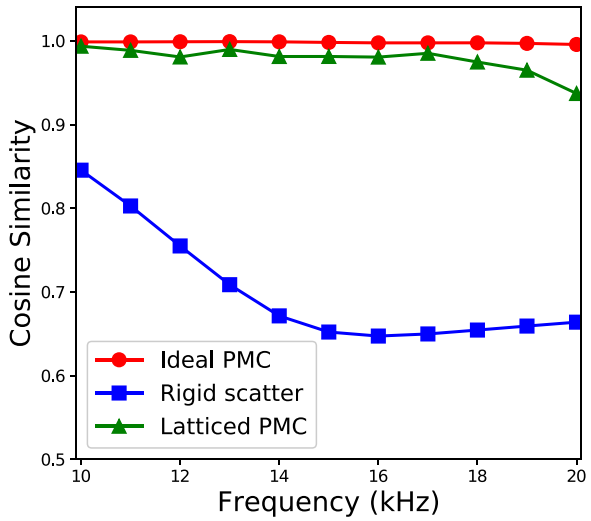

FIG. 5. The CSIs of the theoretical cloak (red circles), rigid scatter (blue squares), and latticed PMC (green triangles) for the waves incident at 55°.

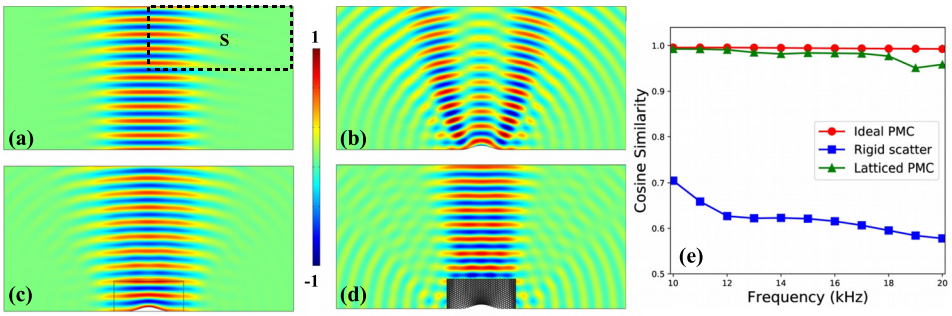

FIG. 6. The scattered acoustic pressure of (a) the rigid plane, (b) the rigid scatter, (c) the theoretical cloak, and (d) the latticed PMC at 15 kHz incident in the vertical direction. (e) The CSIs of the theoretical carpet cloak (red circles), rigid scatter (blue squares), and latticed PMC (green triangles).

is obvious that in the vertical incident case, the latticed PMC exhibits the cloak behavior as good as that in the oblique incident case.

In conclusion, we design a latticed PMC via the QCT method. The QCT has been used twice: the first time is to calculate the required parameters of the designed cloak; the second time is to deform the PM array to the carpet cloak. The performance of the latticed PMC is evaluated by full wave numerical simulation. The CSIs are calculated, which shows that the latticed PMC has an almost perfect effect to conceal the bump in a broadband frequency domain. This confirms the validation of the QCT method in carpet cloak design and unit cell deformation. This work provides a feasible method to realize a quasi-isotropic underwater carpet cloak, which has potential application in underwater acoustic detection. Furthermore, the deformation technique may have potential values for the design of arbitrary shaped devices.

The authors sincerely acknowledge the financial support of the National Natural Science Foundation of China (Grant No. 11874383), the Youth Innovation Promotion Association CAS (Grant No. 2017029), and the IACAS Young Elite Researcher Project (Grant No. QNYC201719).

REFERENCES

[1]J. B. Pendry, Science **312**, 1780 (2006).
[2]U. Leonhardt, Science **312**, 1777 (2006).
[3]S. A. Cummer and D. Schurig, New J. Phys. **9**, 45 (2007).
[4]H. Chen and C. T. Chan, Appl. Phys. Lett. **91**, 183518 (2007).
[5]J. B. Pendry and J. Li, New J. Phys. **10**, 115032 (2008).
[6]B.-I. Popa and S. A. Cummer, Phys. Rev. B **83**, 224304 (2011).
[7]W. Hu, Y. Fan, P. Ji, and J. Yang, J. Appl. Phys. **113**, 024911 (2013).
[8]L. Zigoneanu, B.-I. Popa, and S. A. Cummer, Nat. Mater. **13**, 352 (2014).
[9]J. Zhu, T. Chen, Q. Liang, X. Wang, J. Xiong, and P. Jiang, J. Phys. D: Appl. Phys. **48**, 305502 (2015).
[10]Y. Bi, H. Jia, W. Lu, P. Ji, and J. Yang, Sci. Rep. **7**, 705 (2017).
[11]Y. Bi, H. Jia, Z. Sun, Y. Yang, H. Zhao, and J. Yang, Appl. Phys. Lett. **112**, 223502 (2018).
[12]J. Li and J. B. Pendry, Phys. Rev. Lett. **101**, 203901 (2008).
[13]Z. Chang, X. Zhou, J. Hu, and G. Hu, Opt. Express **18**, 6089 (2010).
[14]G. W. Milton and A. V. Cherkaev, J. Eng. Mater. Technol. **117**, 483 (1995).
[15]A. N. Norris, J. Acoust. Soc. Am. **125**, 839 (2009).
[16]A.-C. Hladky-Hennion, J. O. Vasseur, G. Haw, C. Croënne, L. Haumesser, and A. N. Norris, Appl. Phys. Lett. **102**, 144103 (2013).
[17]M. Kadic, T. Bückmann, N. Stenger, M. Thiel, and M. Wegener, Appl. Phys. Lett. **100**, 191901 (2012).
[18]R. Hedayati, A. M. Leeflang, and A. A. Zadpoor, Appl. Phys. Lett. **110**, 091905 (2017).
[19]Y. Tian, Q. Wei, Y. Cheng, Z. Xu, and X. Liu, Appl. Phys. Lett. **107**, 221906 (2015).
[20]Y. Chen, X. Liu, and G. Hu, Sci. Rep. **5**, 15745 (2015).
[21]X. Cai, L. Wang, Z. Zhao, A. Zhao, X. Zhang, T. Wu, and H. Chen, Appl. Phys. Lett. **109**, 131904 (2016).
[22]A. Zhao, Z. Zhao, X. Zhang, X. Cai, L. Wang, T. Wu, and H. Chen, Appl. Phys. Lett. **110**, 011907 (2017).
[23]X. Su, A. N. Norris, C. W. Cushing, M. R. Haberman, and P. S. Wilson, J. Acoust. Soc. Am. **141**, 4408 (2017).
[24]Y. Chen, M. Zheng, X. Liu, Y. Bi, Z. Sun, P. Xiang, J. Yang, and G. Hu, Phys. Rev. B **95**, 180104 (2017).
[25]Z. Sun, H. Jia, Y. Chen, Z. Wang, and J. Yang, J. Acoust. Soc. Am. **143**, 1029 (2018).
[26]C. Ren, Z. Xiang, and Z. Cen, Appl. Phys. Lett. **97**, 044101 (2010).
[27]Z. Chang, J. Hu, G. Hu, R. Tao, and Y. Wang, Appl. Phys. Lett. **98**, 121904 (2011).
[28]A. N. Norris, Proc. R. Soc. A **470**, 20140522 (2014).
[29]A. A. Kutsenko, A. J. Nagy, X. Su, A. L. Shuvalov, and A. N. Norris, Q. J. Mech. Appl. Math. **70**, 131 (2017).
[30]B. Zhang, T. Chan, and B. Wu, Phys. Rev. Lett. **104**, 233903 (2010).